Advanced Acoustic Simulation of Aircraft and Spacecraft Test Environments: Integration of The Direct Field Acoustic Testing Methodology

Alexis Castel[1], Adam Weston[2], Satya Deshpande[3], Bryce Gardner[4], Rabah Hadjit[5]
ESI Group
32605 W 12 Mile Rd Ste 350,
Farmington Hills, MI 48334

ABSTRACT

In aeroacoustic engineering, replicating real-world environments in a controlled setting presents significant opportunities for reduced flight testing but also comes with challenges when precisely simulating the flight environment. This paper introduces an innovative acoustic simulation model that leverages the Boundary Element Method (BEM) and a Direct Field Acoustic Testing (DFAT) simulation module. The primary objective is to virtually reproduce test sound fields that closely mimic the full fluctuating pressure environments aircraft encounter during flight using only loudspeaker arrays.

This approach involves virtually reproducing a sophisticated test setup, typically comprising hundreds of drivers actively managed to generate a specific sound field. This setup is designed to virtually replicate various complex pressure environments, such as those produced by a Turbulent Boundary Layer, the complex pressure fields generated by aircraft propellers or jet engines. The use of active noise generation simulation helps determine the feasibility of a given pressure field and the capability of a test facility to simulate it accurately.

The virtually reproduced sound fields simulated by this model show remarkable potential in approximating real-world pressure loadings. This capability is particularly useful in establishing pre-test predictions for fuselage testing such as sidewall build-ups: including insulation, and damping treatments, tuned vibration absorbers (TVAs) and tuned mass dampers (TMDs).

This approach also offers a reliable method for anticipating and mitigating unwanted acoustic phenomena occurring during test by accounting for things such as room acoustics and testing fixture dynamics.

[1] alexis.castel@esi-group.com,

[2] adam.weston@esi-group.com

[3] satya.deshpande@esi-group.com

[4] bryce.gardner@esi-group.com

[5] rabah.hadjit@esi-group.com

1. INTRODUCTION

Recent developments in engineering practices have made the use of computer-aided technology for product development irreplaceable. As the engineering world is moving away from physical prototyping, the necessity of simulating test environments is increasing day by day. During the product design and development phase, analytical loads are used as design parameters and constraints. To quantify the performance of the virtual part developed, simulating the virtual test environment is a necessity.

Easy access to high-speed computing and evolution of the complex active control systems have allowed to control of larger frequency bands. Initially developed for active noise cancellation systems, these techniques are being used for controlling an acoustic field in an open space. By constraining measured locations to precise levels and relative coherence allows for Direct Field Acoustic Testing (DFAT). This also allows for a portable high-intensity acoustic test system for the qualification of aerospace components which are replacing the traditional reverberant chamber tests. To conduct this DFAT, stacks of speakers are placed around the test article and a controller produces a sound field based on the levels measured by control microphones placed around the test article. Additional monitor microphones are usually also placed around the structure to ensure required levels are met at a larger number of locations around the structure. The method [1] has been widely accepted and used in the structural qualification process by multiple spacecraft and launch vehicle manufacturers including NASA, ESA, etc.
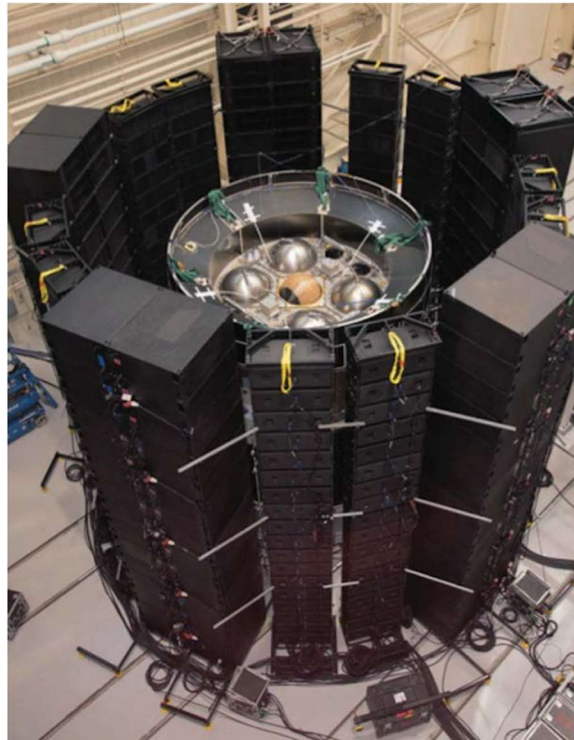

Figure 1: NASA DFAT setup (Image credit: NASA.gov) [2]

As the test article increases in size or complexity, conducting a DFAT can be a high-stakes affair. In order to make DFAT a successful proposition, developing a DFAT simulation promises to provide guidelines for an effective and efficient progression and result in time savings during the test. These simulation methods have recently been developed and provide a definite and validated technique to model the sound field from a DFAT. A Diffuse Acoustic Field (DAF) can be replicated as a summation

of incoherent plane waves impacting the test article from all directions. This approach is the standard modeling method to simulate reverberant room tests. Of course, this is subjected to low-frequency assumptions dependent on room size and shape. However, this simplified representation is not applicable for modeling the more complex acoustic field created by the speaker stacks around the structure and the control loop used in DFAT. Additional reflections and standing waves are produced by the stacks of speakers and the test article. Some incidence angles have varying amounts of acoustic power due to deviations in the direct path between the source and the test article. Boundary Element Method (BEM) is usually preferred to model a reverberant field in a large unbounded volume and has demonstrated promising abilities to simulate the DFAT field.[3][4][5][6] Furthermore, simulation can play an important role for DFAT; in addition to predicting structural response, it also has been used to either optimize the test setup or to ensure the acoustic field will possess the right characteristics such as amplitude, diffusivity, as well as avoiding hot spots or low sports.

Drawing inspiration from the spacecraft industry, aircraft manufacturers have implemented DFAT techniques for conducting experiments on a fuselage. One such experiment employed a loudspeaker array (LSA) to generate counter-rotating open rotor (CROR) engine harmonics to study the corresponding fuselage pressure distribution. [7] The experimental setup also included active digital signal processing (DSP) from the microphone signals and the excitation frequencies. The microphone signals were used as feedback signals for the control algorithm, while the frequencies of the LSA were used for the harmonic reference signal synthesis. This paper expands on these concepts and proposes a test simulation for the aircraft industry, adapting its concepts to the test setup discussed beforehand.
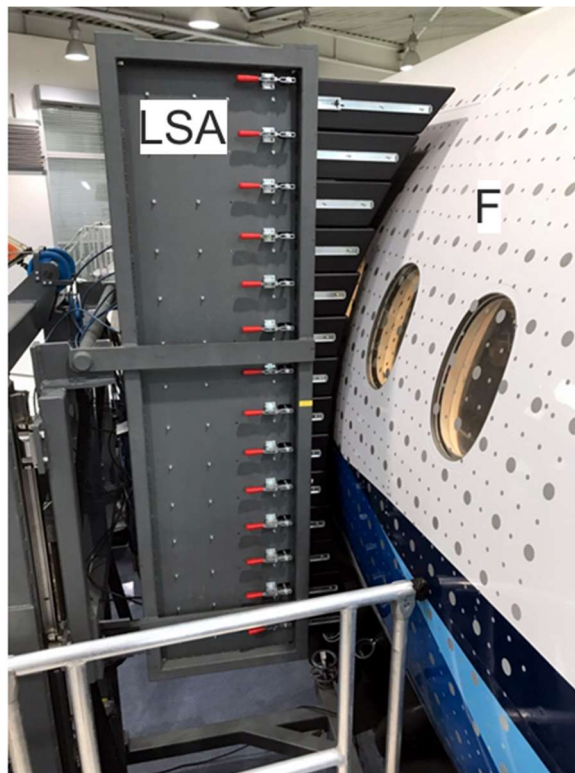

Figure 2: Experimental setup with loudspeaker array (LSA), aircraft fuselage (F)
(Image credit: Institute of Composite Structures and Adaptive Systems
Braunschweig, Germany)

2. ACTIVE NOISE GENERATION SIMULATION PRINCIPLES

This section describes the essential concepts of active noise control generation simulation as implemented in the Direct Field Acoustic Testing simulation module for VA One.

Boundary Element Model Components

Virtual test reproduction aims at integrating every relevant component from the test, these include:
- the test article,
- the noise generation system, here a speaker bank,
- all microphones used for controlling or monitoring the levels,
- additional relevant components of the test such as
  - Ground support equipment,
  - The test room itself.

Here the sources are modeled as normal velocity constraints, meaning individual sets of boundary elements where a Neumann boundary condition is set.

In order to account for all of these elements, the Boundary Element Method (BEM) is chosen as the method of choice as it limits the amount of meshing work necessary, and the solver is set in a way that the transfer function between:
- every source and microphone (both control and monitor microphones)
- every source and structural node

These transfer functions can be arranged into matrices noted $[H_{ij}]$ with i representing the microphone index and j the microphone or surface node location index.

Given this information, we can simulate an active noise generation system such as the one used in the Direct Field Acoustic Testing setup. For this we set an array of microphones where we have a known sound field target defined as a frequency-dependent cross-spectral we will note $[S_{pp}]$. Note that here, the matrix is of size n_microphones x n_microphones values on the diagonal represent the amplitude squared on each microphone while the off-diagonal terms represent the cross-correlation between any two microphones.

Similarly, we can define another cross-spectral matrix defining the excitation for each speaker noted $[S_{vv}]$.

Active noise generation basics

Using the previously defined matrices, we can relate all of them with the following expression:

$$[S_{pp}]_{effective} = [H_{ij}][S_{vv}][H_{ij}]^H \tag{1}$$

where $[\ ]^H$ notes the transpose conjugate of the matrix

Provided we have the same number of drivers and microphones, we can invert this expression and write

$$[S_{vv}] = [H_{ij}]^{-1}[S_{pp}]_{target}[H_{ij}]^{-H} \tag{2}$$

This allows us to calculate a desired excitation when given an idealized $[S_{pp}]$ matrix. Section 0 details the equations defining $[S_{pp}]$ for a turbulent boundary layer pressure field.

However, commonly such an active system is run with a square controller, meaning that there are more control microphones than independent channels coming out of the controller. The system is over-

constrained and becomes a least square invert problem. This is useful when ensuring that the sound field is uniform and not simply controlled at the microphone locations. in this case equation (2) becomes

$$[S_{vv}] = pinv([H_{ij}])[S_{pp}]_{target} pinv([H_{ij}]^H)$$ (3)

Optimization and advanced concepts

When performing a test, one may choose to give more importance to the sound amplitude target. Later development of the algorithm uses a gradient-based optimization algorithm with an objective function $f([S_{vv}])$ defined as a combination of both the amplitude $f'([S_{vv}])$ and cross-correlation $f''([S_{vv}])$. We then introduce a λ factor to help define this objective function.

$$f([S_{vv}]) = \lambda f'([S_{vv}]) + (1 - \lambda) f''([S_{vv}])$$ (4)

Although the specifics of $f'([S_{vv}])$ and $f''([S_{vv}])$ are not defined in this paper, those are objective functions related to the difference between a $[S_{pp}]_{target}$ and $[S_{pp}]_{effective}$ where the value of $f([S_{vv}])$ lowers as the difference between a $[S_{pp}]_{target}$ and $[S_{pp}]_{effective}$ reduces.

Additionally, one may need to correlate different drivers together to represent the effective wiring between the speakers and the controller during the test. This is done by introducing a coupling matrix $[M]$ containing zeros and ones to represent such coupling. In that case, equation (3) becomes

$$[S_{vv}] = pinv([H_{ij}])[M][S_{pp}]_{target}[M]^T pinv([H_{ij}]^H)$$ (5)

The finality of the setup is to represent the specificities of the test, whether they are set in the controller (amplitude target vs cross-correlation) or physical (wiring).

3. SIMULATION EXAMPLE SETUP

As the objective of this model is to reproduce the test setup described in the introduction, the model reproduces a similar setup with all major components while using a generic structure. The following details the specifics of the proposed model:

Structure and acoustic boundary conditions

The studied structure represents a 6-meter diameter fuselage section and is 5 meters long. In order to limit the number of structural modes and as the model is aiming at exciting a small region of the model, the flexible structure is effectively a 2-meter side length curved panel with simply supported boundary conditions. The shell properties are set to be a 1 mm thick Aluminum shell. Outside of the flexible shell, the cylinder is considered a rigid boundary condition.
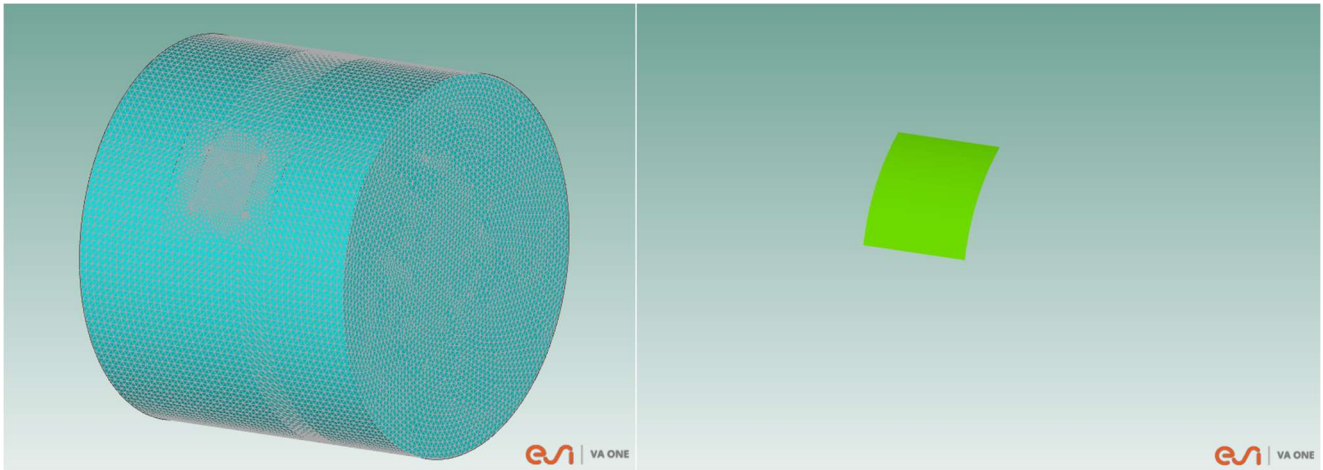
Figure 3: Fuselage section representation (left) and flexible subsection (right)

Coupled model

As described in the previous section, the Boundary Element Method (BEM) is used to model the acoustic field around the cylinder and the active generation system. An array of 10 by 10 individual faces (10 cm side length each representing a speaker where a velocity constraint is placed) are added to the cylinder description described in the previous paragraph.
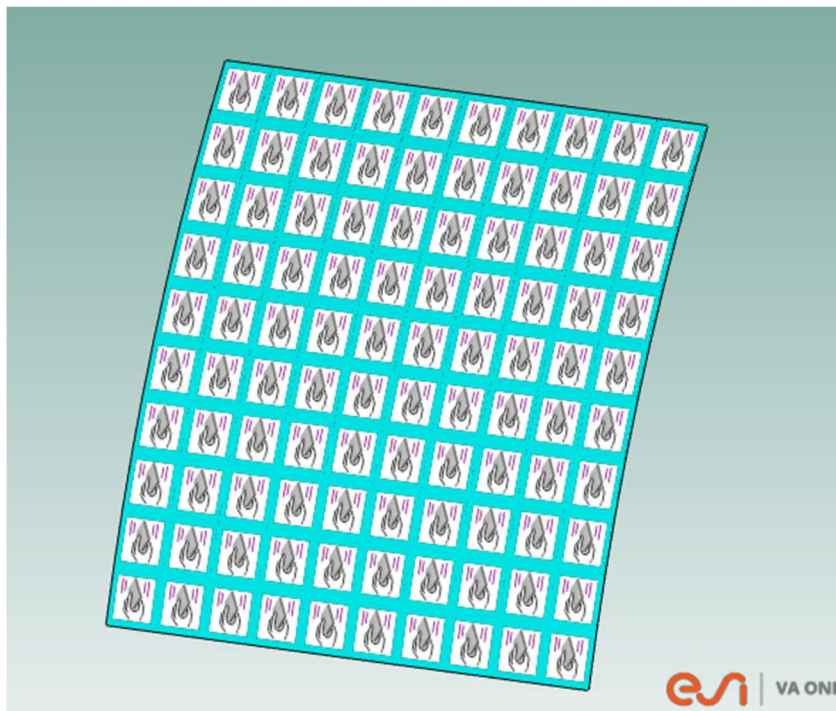

Figure 4: Array of 100 drivers

The BEM fluid then contains a total of 13733 wetted nodes. To this, 360 acoustic sensors are added (Figure 5):
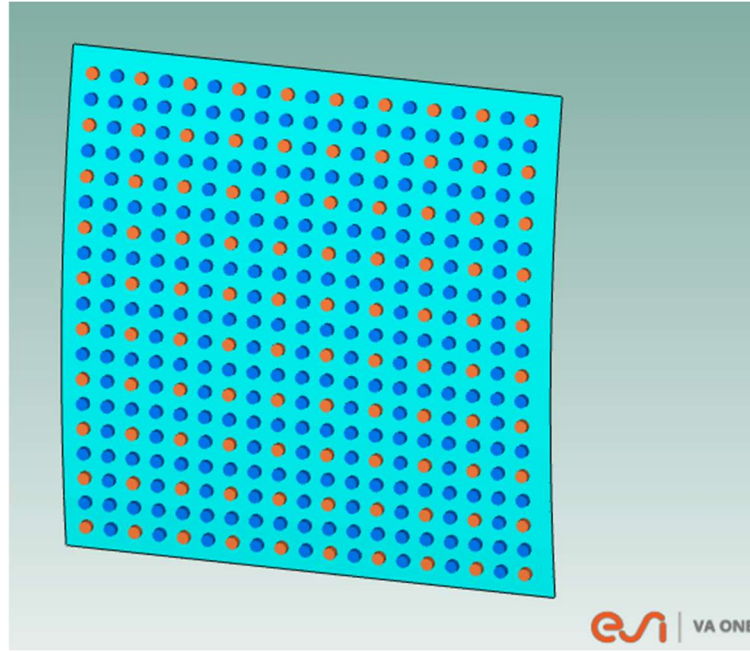
Figure 5: Array of 360 microphones – Divided in two sets: one microphone per driver (orange) and 260 additional microphones (blue).

The two sensor sets presented above allow for either a square control (as presented in equation (2)) or a rectangular control (as presented in equation (3)). For the purpose of active noise generation, the BEM solver here calculates the transfer functions between every driver and every microphone as well as those between every driver and the modal response.

Turbulent Boundary Layer sound field

In order to perform an active noise generation study, we must determine $[S_{pp}]_{target}$. While a diffuse acoustic field is a typical target, for an aircraft, one can set $[S_{pp}]_{target}$ to be a Corcos Turbulent Boundary Layer (TBL), for this, we use the model described in [7], which represents an excitation using the parameters described in the following figure:
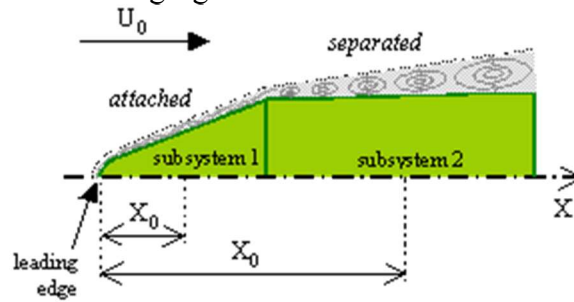

Figure 6: Parameters of a turbulent boundary layer. (U0 – Free Stream Flow Velocity, ρ – Fluid Density c0 – Fluid Speed of Sound, δ – Turbulent Boundary Layer Thickness, X0 – Distance from the leading edge of the TBL to the center of the pressure load on the surface of the subsystem, ν – Fluid Kinematic Viscosity)

The turbulent boundary layer thickness can be computed from the following equations:

$$\delta = 0.37 \frac{X_0}{Re^{0.2}} \text{ with } Re = \frac{U_0 X_0}{\nu} \tag{6}$$

The narrowband spatial correlation function R between two points $\mathbf{x}$ and $\mathbf{x'}$ takes the following normalized form.

$$R(x, x', \omega) = \exp\left[-\frac{c_x|\Delta x|}{d} - \frac{c_y|\Delta y|}{d}\right] \times \exp[-ik_c\Delta x] \text{ with}$$

$$\frac{1}{d} = k_c\sqrt{1 + \left(\frac{8}{3k_c\delta}\right)^2} \tag{7}$$

The second term in the square root above is a correction to the decaying terms that accounts for cases where the boundary layer thickness is small compared to the convection wavelength ($k_c\delta \ll 1$). This correction is not used in this study.

Where the dimensionless parameters c_x and c_y are the spatial correlation coefficients of decay in the *along-flow* and *cross-flow* directions, Δx and Δy are *along-flow* and *cross-flow* signed distances between points, and k_c is the convection wavenumber. The convection wavenumber can be directly specified or computed from the convection velocity using the following equation.

$$k_c = \frac{\omega}{U_c} \tag{8}$$

For this study, we are considering the flow to be attached, therefore, we use:

$$S_p(f) = \frac{p_{RMS}^2}{f_0\left(1 + \left(\frac{f}{f_0}\right)^A\right)^B} \tag{9}$$

With A = 0.9, B = 2.0 and C = 0.346.

Additionally: $\frac{p_{RMS}}{q} = \frac{0.006}{1+0.14M^2}$, $q = \frac{1}{2}\rho U_0^2$, $M = \frac{U_0}{c_0}$ and $f_0 = C\frac{U_0}{\delta}$.

For this model, we arbitrarily chose the standard Air property at sea level and flow velocity of 300 m/s and X_0 = 5 m. Additionally, reference [8] gives us reference values of c_x=0.72, c_y=0.10.

4. VERIFICATION MODEL

The TBL loading described in the paragraph above is a standard load that can be directly applied to the structure and is often a standard load in acoustic simulation software. Therefore, a reference model is created in VA One where an identical structure is subject to a TBL load with the same parameters as the one used to calculate $[S_{pp}]_{target}$. For this study, we chose to remove the boundary layer thickness correction detailed in equation (7).

Additionally, a Semi-Infinite Fluid is placed to represent the effect of air on the structure by adding a reactive and resistive impedance on the structure. The figure below shows the area in blue which matches the speaker excitation area and the green area outside of the speaker excitation.
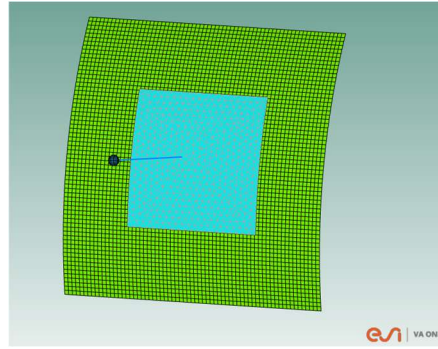
Figure 7: Verification model – The area in blue represents the excited area which matches the area in front of the drivers in the coupled FE-BEM model.

5. RESULTS

Using the models described above, each model is solved from 15.625 Hz to 500 Hz using a 1/36th Octave Band frequency step. Solving this model is therefore a multiple-step process so that it is both coupled between FE and Acoustics as well as properly modeling the active noise generation system:

- A total of 208 structural models are solved up to 600 Hz.
- A BEM solver is used to obtain the transfer functions previously described.
- $[S_{vv}]$ is then calculated for a target $[S_{pp}]$ representing a TBL. For simplicity, equation (3) is used and no optimization algorithm is specified.
- The coupled FE-BEM model is then solved.

Following this, the two primary output quantities that can easily be observed are the sound pressure level at and around the control microphones as well as the structural response of the panel.

Generated sound field

When looking at the generated sound field in the form of a contour plot (figure below) we see a very uniform and controlled level as the location of the control microphones and a variation outside of the control microphone locations.
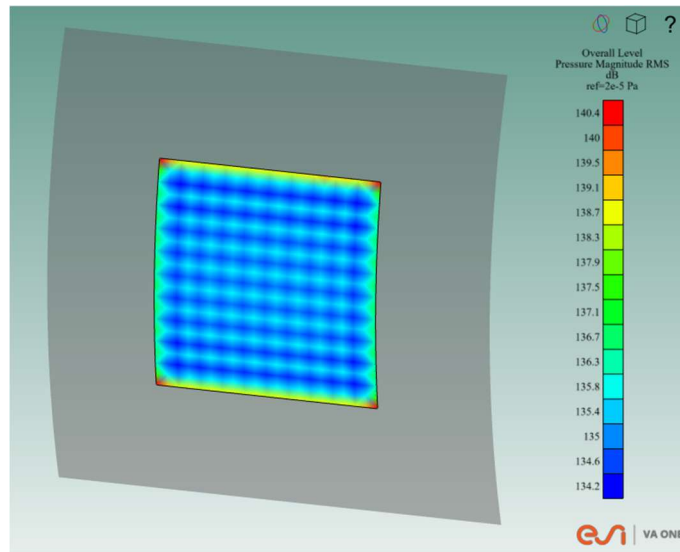

Figure 8: Contour plot of the overall sound pressure level

When comparing the pressure response at a given microphone, the pressure calculated at a given microphone is matching exactly the pressure specified by the analytical load:
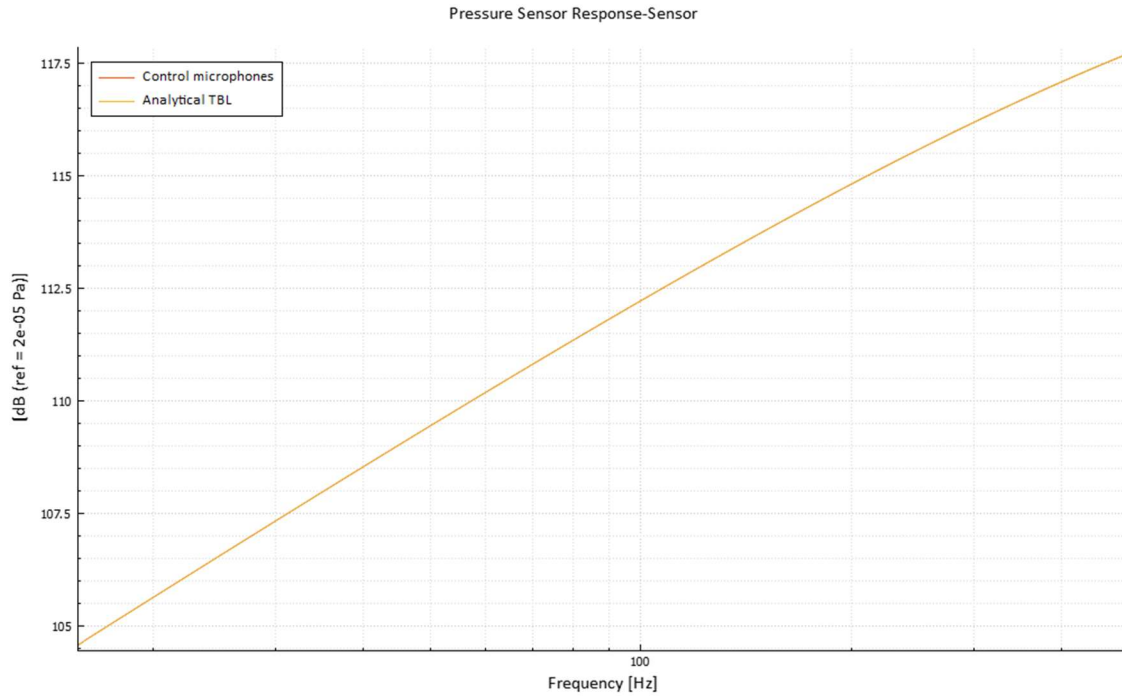
Figure 9: Pressure response at a control microphone vs target pressure spectrum for a square control.

This is because, for this initial calculation, the number of microphones matches exactly the number of drivers. The system is therefore square and no least square approximation is performed.

When using all 360 sensors, the system is over-constrained and more locations are used to target the sound field. In this case, we expect the small difference between the target pressure and the effective pressure at a microphone may differ from the target as shown in the figure below.
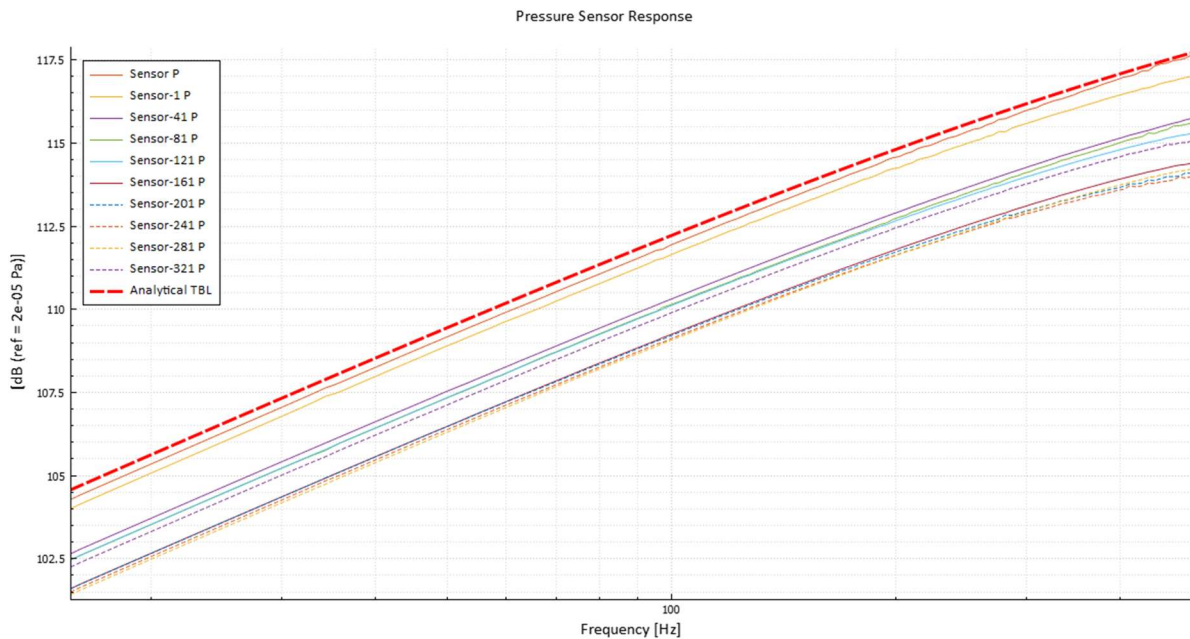

Figure 10: Pressure response at a control microphone vs target pressure spectrum for a rectangular control

We note here that the levels on the randomly chosen microphone are systematically slightly below the target. This can be improved by using the strategy proposed in section 0.

Structural Response

The following graph compares the average structural response of the verification model described in section 4 to that obtained with the active noise generation simulation model using 360 control microphones. We can see that generally, both curves are similar in shape we still observe large differences in levels. While these differences are linked to the profound difference in methodology between both simulation methods, the number of drivers and their individual sizes is expected to play a major role in the high-frequency range as the convective wavelength becomes smaller in the high-frequency range.

Above 300 Hz, we note that both curves are converging towards each other, we can hypothesize that for large wavelengths, it may be more difficult to control the excitation with a given set a limited set of drivers of physical drivers at a fixed distance from the test article.

Additionally, while the contour plots show substantial differences when comparing the overall levels, we do see matching trends when comparing responses at the higher end of the studied frequency range. This is illustrated by Figures 11 and 12. The differences in the overall level for the whole frequency range could be explained in the representation of the test setup where the drivers may excite the structure outside of the target area and therefore raise the vibration response of the panel. The effect tends to be limited in the high-frequency range, as the acoustic wavelength is smaller and the sound pressure level control is more of a local effect.
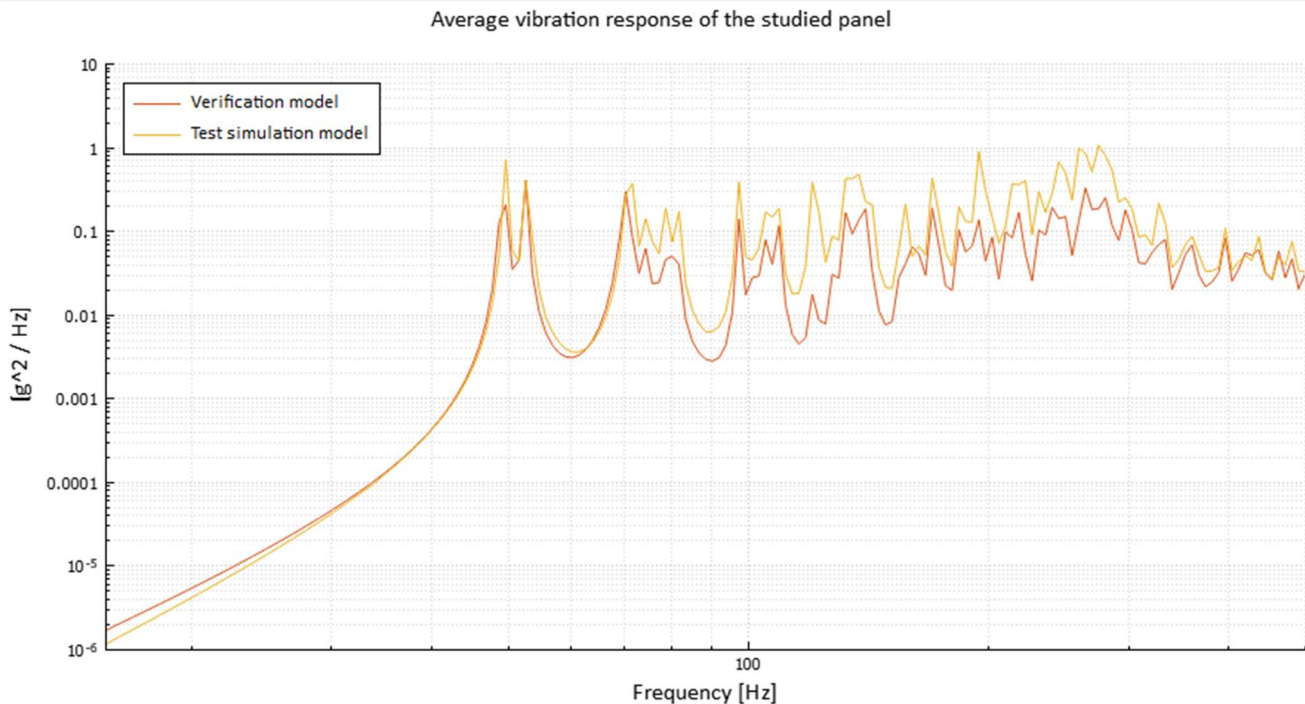

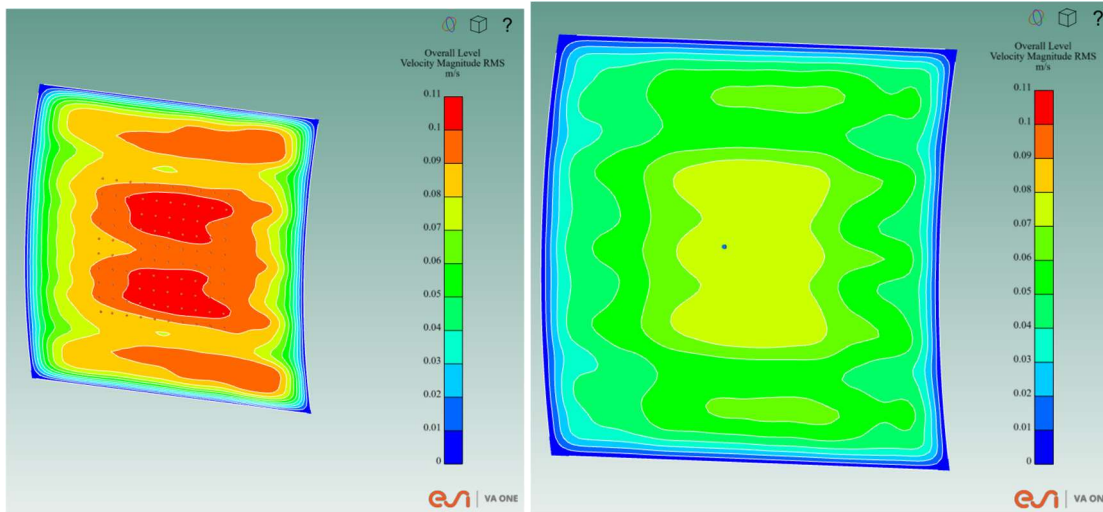Figure 11: Average structural velocity response

Figure 12: Contour plot of the overall vibration response – Test simulation model on the left, empirical TBL verification model on the right.
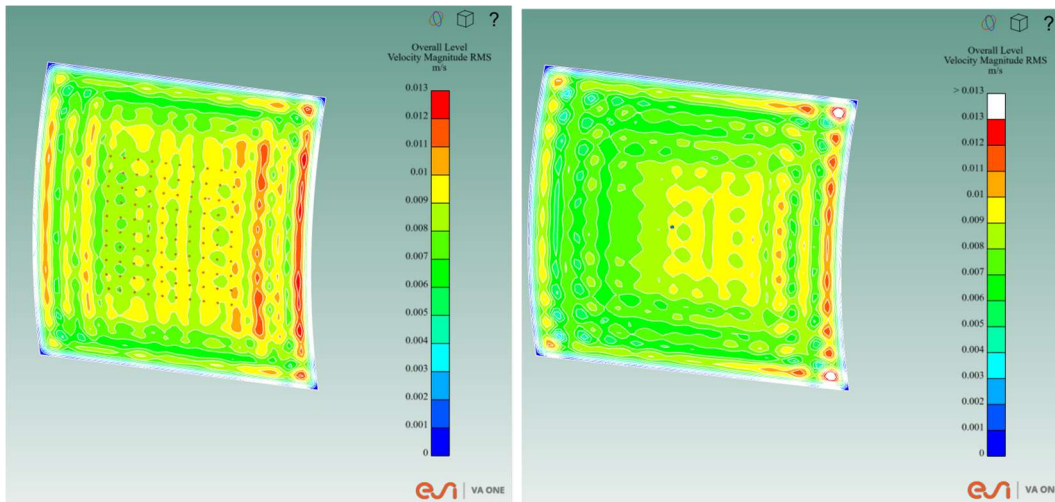

Figure 13: Contour plot of the cumulative vibration response from 400 Hz to 500 Hz – Test simulation model on the left, empirical TBL verification model on the right.

6. CONCLUSIONS AND FUTURE WORK

This paper demonstrates extending some of the existing capabilities of the VA One DFAT simulation tool into new areas of aerospace simulation beyond the direct field acoustic testing realm. The initial results for the TBL simulation are good for the exterior pressure spectra match and are close for the structural response as well.

Future development for this technique will focus on several key areas. The first is the refinement of the algorithm to match the acoustic levels. There is a number of active control algorithms that could be investigated to determine the best solution for each aero source. Control algorithms could also prioritize cross-correlation over absolute pressure level.

The modeling could also use accelerometer sensors for control rather than microphones to better match the structural response of the analytical model. Another area for additional focus is exploring wavenumber post-processing to validate the generated sound field. This can lend insight into better structural acoustic characteristics. The inclusion of validation testing in a representative test facility would be ideal to identify any additional test-specific discrepancies that should be captured in this modeling approach.

7. REFERENCES

1. NASA, "NASA-HDBK-7010: DIRECT FIELD ACOUSTIC TESTING (DFAT)," NASA Technical Handbook, 2016
2. Johnson, A.; Lawson, R.; Fogt, V.; Fiorelli, K.; Bremner, P. "Investigation of Multi-Input, Multi-Output (MIMO) Random Control Applied to Direct Field Acoustic Testing " NASA Spacecraft and Launch Vehicle Dynamic Environments Workshop, June 2018
3. C. Fabries, B. Bertrand, S. Clamagirand, "Direct Field Testing Simulation for Subsystem Acoustic Qualification," in Proceedings of 2016 ECSSMET Conference, Toulouse, France, 2016.
4. B. Gardner, V. Cotoni and A. Kolaini, "Investigation of Direct Field Acoustic Testing with BEM," in SCLV, El Segundo, CA, 2012.
5. B. Gardner, "Investigating DFAT Diffusivity Using Wavenumber-Frequency Analysis with Boundary Element Models," in SCLV, El Segundo, CA, 2017.
6. I. Dandaroy, "Analytical Tool for Numerically Simulating a Direct Field Acoustic Test," in SCLV, El Segundo, CA, 2017.
7. Misol, M. "Active sidewall panels with virtual microphones for aircraft interior noise reduction." Applied Sciences 10.19 (2020): 6828.
8. Cockburn, J.A., Robertson J.E. "Vibration Response of Spacecraft Shrouds to In-flight Fluctuating Pressures," Journal of Sound and Vibration, 1974, 33(4), 399-425.
9. Rennison, D.C., Piersol, A.G., Wilby J.F., Wilby E.G."A review of the Acoustic and Aerodynamic Loads and the Vibration Response of the Space Shuttle Orbiter Vehicle," STS-1 Dynamics Verification Assessment - BBN Report 4438 for NASA, Jet Propulsion Laboratory, November 1980.